ASE Noise Simulation in Raman Amplification Systems

Nelson J. Muga*†, Meire C. Fugihara*‡, Mário F. S. Ferreira† and Armando Nolasco Pinto*‡
*Instituto de Telecomunicações, 3810-193 Aveiro, Portugal.
†Departamento de Física, Universidade de Aveiro, 3810-193 Aveiro, Portugal.
‡Departamento de Electrónica, Telecomunicações e Informática, Universidade de Aveiro, 3810-193 Aveiro, Portugal.
Emails: muga@av.it.pt, meire@av.it.pt, mfernando@ua.pt and anp@ua.pt.

***Abstract*—A method to generate non-white noise is proposed. Using this method, a model accurately describing the amplified spontaneous emission noise in systems with distributed Raman gain is presented. Numerical simulations for the amplified spontaneous emission noise power spectrum were corroborated with experimental results.**

***Index Terms*—Amplified spontaneous emission, non-white noise, optical noise, Raman amplification.**

I. Introduction

In the recent years, telecommunications transport networks capacity has been continuously increased. This has been achieved by increasing the bit rate per channel and by increasing the number of optical channels per fiber [1]. In order to support those systems, broadband optical amplifiers are required. In this context, Raman amplification presents some attractive features when compared with other optical amplification solutions [2], [3].

Optical amplification is an intrinsic source of noise due to the amplified spontaneous emission (ASE) [1]. The noise has direct and multiple implications on the performance of optical communication systems: it degrades the signal-to-noise ratio [1] and induces timing jitter and frequency fluctuations [4], [5], [6]. Therefore an accurate description of the ASE noise is crucial to assess optical fiber communication systems.

In general, simulation, analysis, design and optimization of optical Raman amplification systems are done through the resolution of a system of coupled differential equations for the mean powers of all involved pumps and signals [7], [8], [9]. Nevertheless, even for moderate intensity fields, Kerr effect should also be considered in order to account for the nonlinear fiber response. However, this requires the resolution of the coupled nonlinear Schrödinger equations (NLSEs) for the pump and Stokes fields [10], [11]. The modeling of the spontaneous Raman scattering can be done with the inclusion of a Langevin noise term into the wave equation [10], [12]. Headley and Agrawal have shown that this effect can be considered including a noise term into the third-order nonlinear polarization. Alternative approaches can be used to include the optical noise. For instance, Marcuse has studied the problem adding the ASE noise at the end of each optical amplifier section [13]. After amplification, independent Gaussian random variables are added to each spectral component. However, the noise shape and nonlinear noise-to-noise and noise-to-signal interaction inside the amplifier are ignored in these approaches.

In this work, we present a method to generate frequency-shaped noise and, using that method, we analyze the ASE noise induced by spontaneous Raman scattering in broadband systems. The generalized NLSE is solved through the well-known split-step Fourier method (SSFM) [11] with a non-white noise term added to account for the gain profile [14]. The numerical simulations of our ASE noise model are corroborated with experimental results.

This paper is organized in four sections. In Section II, we present a method to generate non-white noise, which is used in the proposed model for the simulation of the optical noise originated by Raman amplification in optical fibers. Subsequently, we validate experimentally the noise model in Section III. In section IV, the main conclusions are presented.

II. ASE Modeling

A. Wave Equation

Considering the simplest scheme of Raman amplification in optical fibers, based on a single signal and a single pump, with frequencies ω_s and ω_p, respectively, the evolution of the optical field $A_s(z,t)$, which includes signal and noise, can be described by the following equation [15], [16],

$$\begin{aligned}\frac{\partial A_s(z,t)}{\partial z} &= \left(-i\frac{\beta_2}{2}\frac{\partial^2}{\partial t^2} - \frac{1}{2}\alpha_s\right)A_s(z,t) \\ &+ i\gamma[|A_s(t,z)|^2 + (2-f_R)P_p(z)]A_s(z,t) \\ &+ i\gamma f_R P_p(z)\int_{-\infty}^{+\infty} h_R(t-t')A_s(t',z)\exp(-i\Omega_R(t-t'))dt' \\ &+ f_n(z,t), \end{aligned} \quad (1)$$

where α_s is the fiber loss at the frequency ω, $|A_s(z,t)|^2$ is the field power, $\beta_2 = \partial^2\beta/\partial\omega^2$ is the group velocity dispersion coefficient, $P_p(z)$ is the pump average power, γ is the nonlinear coefficient, f_R is the fraction of nonlinearity that arises from the delayed Raman response, Ω_R is the vibrational

This work was supported in part by Fundação para a Ciência e Tecnologia, under the PhD Grant SFRH/BD/28275/2006, and "IP over WDM" project (POSI/EEA-CPS/59566/2004), and by PT Innovation through the "CRT-IT" project (IT-P407)

frequency of the molecules, which is assumed to be at peak of the Raman gain curve, $h_R(t)$ is the Raman response function, and $f_n(z,t)$ is a Langevin noise source [3]. The linear part of (1) includes dispersion and fiber losses, whereas the nonlinear part accounts for signal self-phase modulation, cross-phase modulation and Raman scattering. Note that the Raman gain, $g_R(\Omega)$, is proportional to the imaginary part of the Raman response function, and is defined as $g_R(\Omega) = 2f_R\gamma \mathrm{Im}[\tilde{h}(\Omega)]$, where $\Omega = \omega_p - \omega$, $\tilde{h}_R(\Omega)$ is the Fourier transform of $h_R(t)$ and Im[ ] stands for the imaginary part [11]. The last term in (1), $f_n(z,t)$, represents mathematically the optical noise continuously added through spontaneous scattering.

The noise associated with the spontaneous Raman scattering processes is usually modeled as a white noise process with Gaussian statistics [3]. Using this approximation, the noise represented by $f_n(z,t)$ vanishes on average, $\langle f_n(z,t)\rangle = 0$, and its autocorrelation function is given by [3]

$$\langle f_n(z,t) f_n^*(z',t')\rangle = n_{sp}\hbar\omega_0 g_R(\Omega_0) P_p(z)\delta(z-z')\delta(t-t'), \quad (2)$$

where ω_0 is the central frequency, $\hbar\omega_0$ is the mean photon energy, $\Omega_0 = \omega_p - \omega_0$ represents the Raman shift, i.e. the difference between pump and central frequencies, and n_{sp} is the spontaneous-scattering factor, described by

$$n_{sp}(\Omega_0) = \frac{1}{1-\exp(\frac{-\hbar\Omega_0}{k_B T})}, \quad (3)$$

where k_B is the Boltzmann constant and T is the absolute temperature of the fiber. The delta functions in (2) indicate that, at different positions and times, independent noise events occur.

B. ASE Simulation Using de Split-Step Fourier Method

Without the noise term, equation (1) can be numerically solved using the SSFM [11], which requires the division of the fiber into small steps. For each step, the approximated solution is calculated assuming that the linear and nonlinear effects act independently. Then, in the case of noiseless propagation, we can write

$$\frac{\partial A_s(z,t)}{\partial z} = \left(\hat{D} + \hat{N}\right) A_s(z,t), \quad (4)$$

where $\hat{D}$ and $\hat{N}$ are, respectively, the linear and nonlinear operators. Assuming that $A_s(z,t)$ varies little when compared with the time scale of the Raman response, and that near the gain peak the real part of $\tilde{h}_R(\Omega)$ vanishes, then the term containing the integral on (1) can be written as $1/2\, g_R(\Omega) P_p A_s$ [16]. Therefore, since the linear part of (1) is solved in the frequency domain, we can include the Raman gain term on $\hat{D}$, accounting in this way for the frequency dependence of the gain. The dispersive term of (1) can be written in the frequency domain by replacing the operator $\partial/\partial t$ by $-i\omega$, and therefore the operator $\hat{D}$ becomes

$$\hat{D}(\omega, z) = i\frac{\beta_2}{2}\omega^2 + \frac{1}{2} g_R(\Omega) P_p(z) - \frac{1}{2}\alpha_s. \quad (5)$$

The operator $\hat{N}$ is given by

$$\hat{N}(t,z) = i\gamma\left[|A_s(z,t)|^2 + (2-f_R)P_P(z)\right], \quad (6)$$

and operates in the time domain. Assuming a step Δz, the optical field at the position $z+\Delta z$ can be approximated by

$$A_s(z+\Delta z,t) \cong \exp(\frac{\Delta z}{2}\hat{D}) \times \exp\left[\int_z^{z+\Delta z} \hat{N}(z')dz'\right] \exp(\frac{\Delta z}{2}\hat{D}) A_s(z,t). \quad (7)$$

This solution is a second-order approximation, also called symmetrized SSFM, and has an error proportional to Δz^3 [11].

In order to include the noise term, we add the noise discretely to the field. This means that the noise that is continuously created along a real fiber is approximated by a certain amount of noise that is added to the field at each step of the SSFM. This approximation is reasonable providing that the step Δz is small. For small steps the integral present in (7) can also be approximated by $\exp(\Delta z\hat{N})$. Using these approaches, the total optical field at the position $z+\Delta z$ can be written as

$$A_s(z+\Delta z,t) \cong \exp(\frac{\Delta z}{2}\hat{D}) \times \exp(\Delta z\hat{N}) \exp(\frac{\Delta z}{2}\hat{D}) A_s(z,t) + f(z,t). \quad (8)$$

However, the inclusion of the noise term in (8) reduces the computational efficiency of the SSFM. This occurs because when (8) is applied iteratively, the operation $\exp(\frac{\Delta z}{2}\hat{D})$ do not appear consecutively, therefore only the operator $\hat{N}$ can be applied over the whole step [11]. In order to make the method faster, the position where the noise is added was changed; we start by applying the operator $\hat{D}$ to $A_s(z,t)$ over a distance $\Delta z/2$, after we apply the operator $\hat{N}$ over the whole segment length Δz and, before applying again the operator $\hat{D}$, we add the ASE noise $f_n(z,t)$. Equation (8) is finally written as follows

$$A_s(z+\Delta z,t) \cong \exp(\frac{\Delta z}{2}\hat{D}) \times \left[\exp(\Delta z\hat{N}) \exp(\frac{\Delta z}{2}\hat{D}) A_s(z,t) + f_n(z,t)\right]. \quad (9)$$

Note that if (9) is applied iteratively, the two consecutive operations $\exp(\frac{\Delta z}{2}\hat{D})$ can now be simply replaced by the single operation $\exp(\Delta z\hat{D})$. With this solution we are able to include the noise term on the SSFM, without reducing the numerical efficiency of the SSFM.

C. Non-White Noise Generation

Each spontaneous emission event can be considered independent, therefore $f_n(z,t)$ can be considered as a white Gaussian stochastic process. This means that both real and imaginary components of the field are Gaussian random variables, with variance given by (2). This model are quite suitable if the bandwidth of the simulation is small when compared with the amplifier bandwidth. Note that this approximation ignores the frequency dependence of $g_R(\Omega)$, since the delta

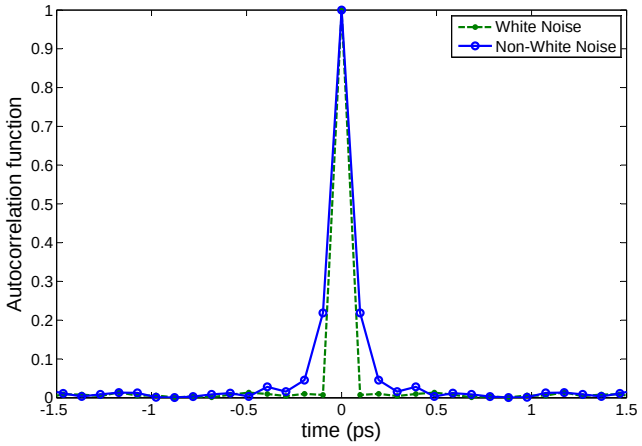

Fig. 1. Autocorrelation function for a white (dashed line) and non-white noise (solid line) distributions. The colorized noise presents a broader autocorrelation function, which indicates an increased correlation between samples of such distribution. The sample period used in the simulations was 0.1 ps.

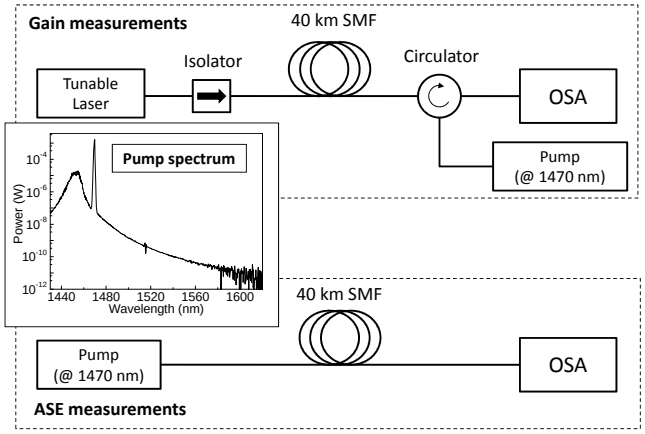

Fig. 2. Experimental setup used to perform the Raman gain coefficient and ASE noise measurements. The inset shows the spectrum of the pump laser used in the setup.

function $\delta(t-t')$ on (2) implies a flat spectrum over all the considered bandwidth [17]. Nevertheless, if the $g_R(\Omega)$ dependence on the frequency is considered, then $f_n(z,t)$ cannot be defined as a white Gaussian noise process. In fact, this consideration becomes relevant for broad bandwidth simulations, where multiple signals at various frequencies are analyzed.

The noise added at each step is z dependent, due to the dependence on the pump power $P_p(z)$, and, at each position, it will be frequency shaped, due to the dependence on the gain profile $g_R(\Omega)$. In our method, the generation of this kind of noise follows three stages:

1) We start by generating a white Gaussian distribution of points, $f_n^w(z,t)$, with mean equal to zero, $\langle f_n(z,t)\rangle = 0$, and variance given by (2) (the superscript w indicates "white" noise). Assuming a finite bandwidth and a small step, the variance is calculated from the following expression

$$\sigma_0^2(z) = n_{sp}(\Omega_0)\hbar\omega_0 g_R(\Omega_0)P_p(z)\Delta z B_{op}, \tag{10}$$

where $g_R(\Omega_0)$ is the Raman gain at the central signal frequency ω_0, Δz is the step used in the SSFM, and B_{op} is the optical bandwidth of our simulation.

2) In the second stage, we perform the Fourier transform of f_n^w, in order to obtain the spectrum of the previously generated distribution,

$$\widetilde{f}^w(z,\omega) = F_T\{f_n^w(z,t)\}, \tag{11}$$

where $F_T\{\,\}$ denotes the Fourier-transform operation. At this point, the obtained spectrum is flat in the considered bandwidth. After that, the spectrum is multiplied by $\sigma_N(z,\omega)$, in order to obtain the desired spectrum profile, i.e. the $g_R(\Omega)$ profile,

$$\widetilde{f}_n^{nw}(z,\omega) = \sigma_N(z,\omega)\widetilde{f}_n^w(z,\omega) \tag{12}$$

where $\sigma_N(z,\omega)$, the normalized standard deviation, is just the ratio between the variances calculated at the frequency ω and central frequency, ω_0,

$$\sigma_N^2(z,\omega) = \frac{n_{sp}(\Omega)\hbar\omega\, g_R(\Omega)P_p(z)\Delta z B_{op}}{\sigma_0^2} \tag{13}$$

$$= \frac{n_{sp}(\Omega)}{n_{sp}(\Omega_0)}\frac{\omega\, g_R(\Omega)}{\omega_0 g_R(\Omega_0)}. \tag{14}$$

In (12) the superscript nw indicates "non-white" noise.

3) Finally, in the third stage, the inverse Fourier transform is performed and a non-white noise, $f_n^{nw}(z,t)$, is obtained in the time domain,

$$f_n^{nw}(z,t) = F_T^{-1}\{\widetilde{f}_n^{nw}(z,\omega)\}, \tag{15}$$

where $F_T^{-1}\{\,\}$ denotes the inverse Fourier-transform operation.

The non-white noise method presented above only changes the "color" of the noise. This means that the colored noise represented by (15) should present the initial distribution, i.e. a Gaussian distribution. On the other hand, changes in the spectral shape induce broadening in the autocorrelation function [18], and therefore (2) is no more verified.

Fig. 1 shows the autocorrelation function for an ensemble of noise samples generated by this method. The autocorrelation function of a standard white noise distribution is also represented in the same figure. The comparison between the two curves shows a broader autocorrelation function of the colorized noise, which indicates an increased correlation between samples of such distribution.

III. Experimental Validation

In order to validate our model, a comparison between simulated and experimental results was performed. The simulation of the ASE noise was based on the numerically resolution of (1), using the modified SSFM and the non-white noise method presented in section II.

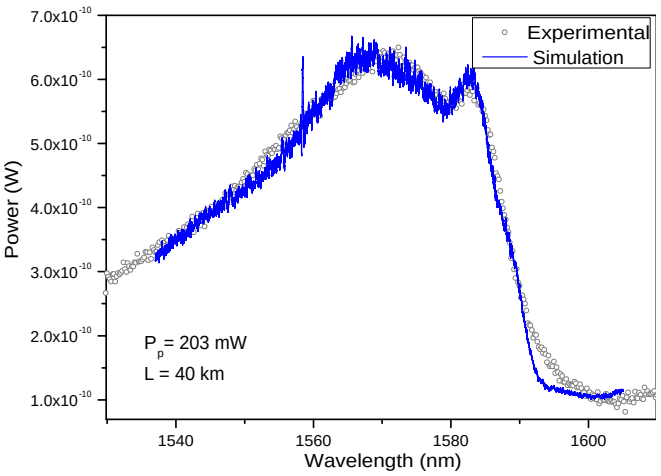

Fig. 3. Experimental and simulated ASE power spectra for a fiber length equal to 40 km and input pump power equal to 203 mW. The Raman pump was centered at 1470 nm and propagated in the forward direction.

The parameters used in the simulations were the following: fiber length equal to 40 km, simulation step size equal to 80 m, nonlinear coefficient of 1.5 $W^{-1}km^{-1}$, group velocity dispersion of -21.4 ps^2/km, fiber losses of 0.23 dB/km, f_R equal to 0.18. We used for $g_R(\Omega)$ a curve resulting from the fit of 14 Gaussian curves to experimental Raman gain values, obtained through on/off gain measurements using the experimental setup depicted in Fig. 2, following the procedure presented in [9] and [14]. Our simulation was centered around the maximum of the gain curve and $A_s(z=0,t) = 0$ and $P_p(z=0,t)$ = 203 mW. The ASE noise power spectral density was obtained from the signal at the fiber output

$$S(\omega) = \frac{\widetilde{A}_s(\omega)\widetilde{A}_s^*(\omega)}{T_W}, \tag{16}$$

where $\widetilde{A}_s(\omega)$ is the Fourier transform of the output signal $A_s(t)$ and T_W is the time window considered in the simulation, which was 12.8 ns. The curve for the ASE noise power was obtained from the convolution of the ASE noise power density spectrum through an ideal filter with bandwidth equal to 15 GHz, and is represented in Fig. 3 as a solid line.

The setup used to perform the experimental ASE noise measurements comprises a semiconductor laser pump, a 40 km single-mode fiber (SMF), and an optical spectrum analyzer (OSA), as schematically represented in Fig. 2. The laser pump was centered at 1470 nm and was propagated in the forward direction with an input power equal to 203 mW. The ASE noise was analyzed at the fiber end in the OSA, and its power spectrum is represented in Fig. 3 as circles. The comparison between the data depicted in Fig. 3 shows a good agreement between simulated and experimental results for the ASE noise. This agreement covers a range of almost 70 nm of the spectrum, i.e., all the simulated bandwidth, which allows us to validate the model.

Since the model presented in this paper accounts for the interaction between signal and ASE noise mediated by the fiber nonlinearities, it can be used, for instance, to assess the changes on the statistics of the ASE noise originated by Raman amplification in optical fiber communication systems.

IV. Conclusion

We have proposed in this paper a method to generate non-white noise, which accounts for the frequency Raman gain profile. Using this method, a non-white noise term was added to the NLSE and a numerical model that accurately describes the ASE noise in optical fiber systems with distributed Raman amplification was presented. The numerical results for the ASE noise power spectrum were validated by results obtained experimentally.

References

[1] G. P. Agrawal, *Fiber-Optic Communication Systems, 3rd edition*. John Wiley & Sons, New York, EUA, 2002.

[2] M. Islam, "Raman amplifiers for telecommunications," *Selected Topics in Quantum Electronics, IEEE Journal of*, vol. 8, no. 3, pp. 548–559, May/Jun 2002.

[3] C. Headley III and G. P. Agrawal, *Raman Amplification in Fiber Optical communication Systems*. Academic Press, EUA, 2004.

[4] A. N. Pinto, G. P. Agrawal, and J. R. F. da Rocha, "Effect of soliton interaction on timing jitter in communication systems," *J. Lightwave Technol.*, vol. 16, no. 4, pp. 515–519, Apr 1998.

[5] A. N. Pinto, J. R. F. da Rocha, Q. Lin, and G. P. Agrawal, "Optical versus electrical dispersion compensation: Role of timing jitter," *J. Lightwave Technol.*, vol. 24, no. 1, pp. 387–395, Jan. 2006.

[6] A. N. Pinto and G. P. Agrawal, "Nonlinear interaction between signal and noise in optical amplifiers," *J. Lightwave Technol.*, vol. 26, no. 13, pp. 1847–1853, Jul 2008.

[7] H. Kidorf, K. Rottwitt, M. Nissov, M. Ma, and E. Rabarijaona, "Pump interactions in a 100-nm bandwidth Raman amplifier," *Photonics Technology Letters, IEEE*, vol. 11, no. 5, pp. 530–532, May 1999.

[8] X. Liu and Y. Li, "Optimizing the bandwidth and noise performance of distributed multi-pump Raman amplifiers," *Opt. Communications*, 2004.

[9] M. Fugihara and A. N. Pinto, "Low-cost Raman amplifier for CWDM systems," *Microwave and Optical Tech. Letters*, vol. 50, pp. 297 – 301, Feb 2008.

[10] C. Headley III and G. P. Agrawal, "Noise characteristics and statistics of picosecond stokes pulses generated in optical fibers through stimulated Raman scattering," *Quantum Electronics, IEEE Journal of*, vol. 31, no. 11, pp. 2058–2067, Nov 1995.

[11] G. P. Agrawal, *Nonlinear Fiber Optics, 3rd ed.* Academic Press, San Diego, EUA, 2001.

[12] M. G. Raymer and J. Mostowski, "Stimulated Raman scattering: Unified treatment of spontaneous initiation and spatial propagation," *Phys. Rev. A*, vol. 24, no. 4, pp. 1980–1993, Oct 1981.

[13] D. Marcuse, "Single-channel operation in very long nonlinear fibers with optical amplifiers at zero dispersion," *Lightwave Technology, Journal of*, vol. 9, no. 3, pp. 356–361, Mar 1991.

[14] N. J. Muga, M. C. Fugihara, Mário F. S. Ferreira, and A. N. Pinto, "Non-Gaussian ASE noise in Raman amplification systems," *accepted for publication in IEEE/OSA J. Lightwave Technol.*, 2009.

[15] G. P. Agrawal, *Applications of Nonlinear Fiber Optics*. Academic Press, San Diego, EUA, 2002.

[16] C. Headley III and G. P. Agrawal, "Unified description of ultrafast stimulated Raman scattering in optical fibers," *J. Opt. Soc. Am. B*, vol. 13, no. 10, p. 2170, 1996.

[17] A. Papoulis, *Probability, random variables, and stochastic processes*. McGraw-Hill, New-York, 1991.

[18] M. C. Jeruchim, P. Balaban, and K. S. Shanmugan, *Simulation of Communication Systems: Modeling, Methodology and Techniques*. Kluwer Academic Publishers, New-York, 2000.